

Solid state synthesis of silver nanowires by biopolymer thin films

By: Rakkiyappan Chandran, Harish Chevva, Zheng Zeng, Yiyang Liu, Wendi Zhang, [Jianjun Wei](#), and [Dennis LaJeunesse](#)

R. Chandran,¹ H. Chevva,¹ Z. Zeng, Y. Liu, W. Zhang, J. Wei, D. LaJeunesse, Solid state synthesis of silver nanowires by biopolymer thin films, *Materials Today Nano*, **2018**, 1, 22-28. DOI: 10.1016/j.mtnano.2018.04.002. (¹equal contribution).

Made available courtesy of Elsevier: <https://doi.org/10.1016/j.mtnano.2018.04.002>



This work is licensed under a [Creative Commons Attribution-NonCommercial-NoDerivatives 4.0 International License](#).

Abstract:

In this paper, we describe a novel method of silver nanowire (AgNW) synthesis. Silver nanoparticles (AgNPs) were synthesized under ambient conditions by a chitosan/chitin-based method. These crystalline AgNPs then served as seeds for the solid-state formation of AgNWs within a drop-cast chitosan/chitin thin film. To the best of our knowledge, this is the first report of AgNW growth on a bio-polymer thin film. Chemical analysis demonstrated that AgNPs and AgNWs produced by this synthetic process have distinct interactions with polysaccharide polymers, and unlike AgNWs produced by other methods, the AgNWs formed in the chitin/chitosan matrix display an irregular twisted morphology. The flexible AgNW/chitosan nanocomposite material is conductive, and we incorporate this new material into a peroxide sensor to demonstrate of its potential applications in chemical sensing devices.

Keywords: Chitin | Chitosan | Silver nanowire | Chemical sensor | Thin film | Polysaccharide

Article:

1. Introduction

Metallic nanoparticles have enhanced and often unique catalytic [1], [2], [3] and physical properties [4], [5]. Silver and other noble metal nanomaterials are of particular interest and importance because of their unique electronic, optical, and biological activities [6], [7], [8], [9]. Silver nanomaterials are synthesized by various methods including photochemical approaches that utilize the light-sensitive aspects of precursor materials, standard chemical approaches using citrate or borate reducing agents, and “green” approaches that use a biological material in at least one step of the synthesis process [10], [11], [12]. Nanoparticle synthetic processes involve several steps that include the reduction of a metal ion in solution into an insoluble precipitate; the formation of a nucleation site either from individual precipitated nanoparticles or by the aggregation of these particles; and the stabilization of the nascent particle, which is followed by the nanoparticle growth [10], [11], [13], [14]. Control of each step enables the control over the size, crystallinity, and morphology of the nanomaterial products from specific synthetic reactions [9], [10], [11], [14], [15].

Several green synthetic methods for generating silver nanoparticles (AgNPs) have also been developed, which use biomolecules such as proteins and polysaccharides to stabilize and promote nucleation [14], [16]. Environmentally friendly “green” methods of nanoparticle synthesis often take advantage of biomimetic self-assembling systems or use catalytic elements such as living cells or biopolymers [13], [17], [18]. A polysaccharide AgNP synthetic method uses starch as the capping agent and monomeric β -d-glucose as the reducing agent in an aqueous solution. Extracts of various plants and microorganisms have also been demonstrated to promote the formation of AgNPs by the participation of protein/peptides in the reduction, nucleation, and stabilization steps [13], [17]. Recently, a chitosan photochemical synthetic method has been described that enables the formation of AgNPs of different morphologies and crystallinities in a wavelength-dependent manner [10]. Synthetic processes that produce highly anisotropically shaped particles are especially desirable in many applications because of the enhancement of specific optical properties such as surface plasmon resonance [9], [12].

Silver nanowires (AgNWs) are synthesized primarily by polyol methods, which are energetically and environmentally costly [13], [16], [19], [20]. Recently, there has been an increased interest in the identification and fabrication of novel nanocomposite materials, which consist of metallic or metal oxide nanoparticles and another nanoscale material [13], [21]. By combining the properties of two nanomaterials, there is often a synergetic effect that extends, enhances, and/or increases the properties of one or more of the constituents of the nanocomposite [22], [23], [24]. However, fabrication methods of such multicomponent nanomaterials often rely on a multistep process, relying on post-fabrication mixing or the combination of individual nanoscale components, which often results in a product that is not ideal in composition and/or non-scalable [25], [26]. In this paper, we describe a novel, single-step process that promotes the self-growth of AgNWs within thin films of the polysaccharide chitin/chitosan. To the best of our knowledge, this is the first report on AgNW growth in solid state. The resulting material is a flexible, conductive biopolymer nanocomposite that has potential in several applications including chemical sensors. Here, we demonstrate the detection of hydrogen peroxide on AgNW/chitosan films by non-enzymatic electrochemistry.

2. Results and discussion

2.1. AgNP synthesis in a chitosan solution

The polysaccharide chitosan is a polymer of β (1 \rightarrow 4)-linked d-glucosamine subunits [27], [28], [29] that has been demonstrated to synthesize AgNPs in aqueous solutions [10], [30]. To synthesize our AgNPs, we produced 5-mM AgNO₃ in a 1% chitosan aqueous solution containing 1% acetic acid; this solution was sonicated for 4 h resulting in a characteristic color change from clear to opaque solution with a purple/pink hue (Fig. 1A). The pH of the chitosan/AgNO₃ solution was 5 during the AgNP synthesis reaction. The maintenance of pH at above 5 is crucial for the synthesis of AgNPs; chitosan/AgNO₃ solutions with a pH of 3 or lower had no AgNP formation (Fig. 2A, left); however, the increase in the pH of the chitosan/AgNO₃ solution to 9 resulted in the formation of a gel state of the chitosan mixture that had the characteristic purple hue of AgNP formation (Fig. 2A, right). SEM analysis of these AgNPs showed the formation of rod-shaped AgNPs instead of cuboidal AgNPs (Fig. 2B). We confirmed the presence of AgNPs

by UV–Vis spectrometry, in which a characteristic AgNP absorption peak appeared at 400–550 nm (Fig. 1B) [13], [15].

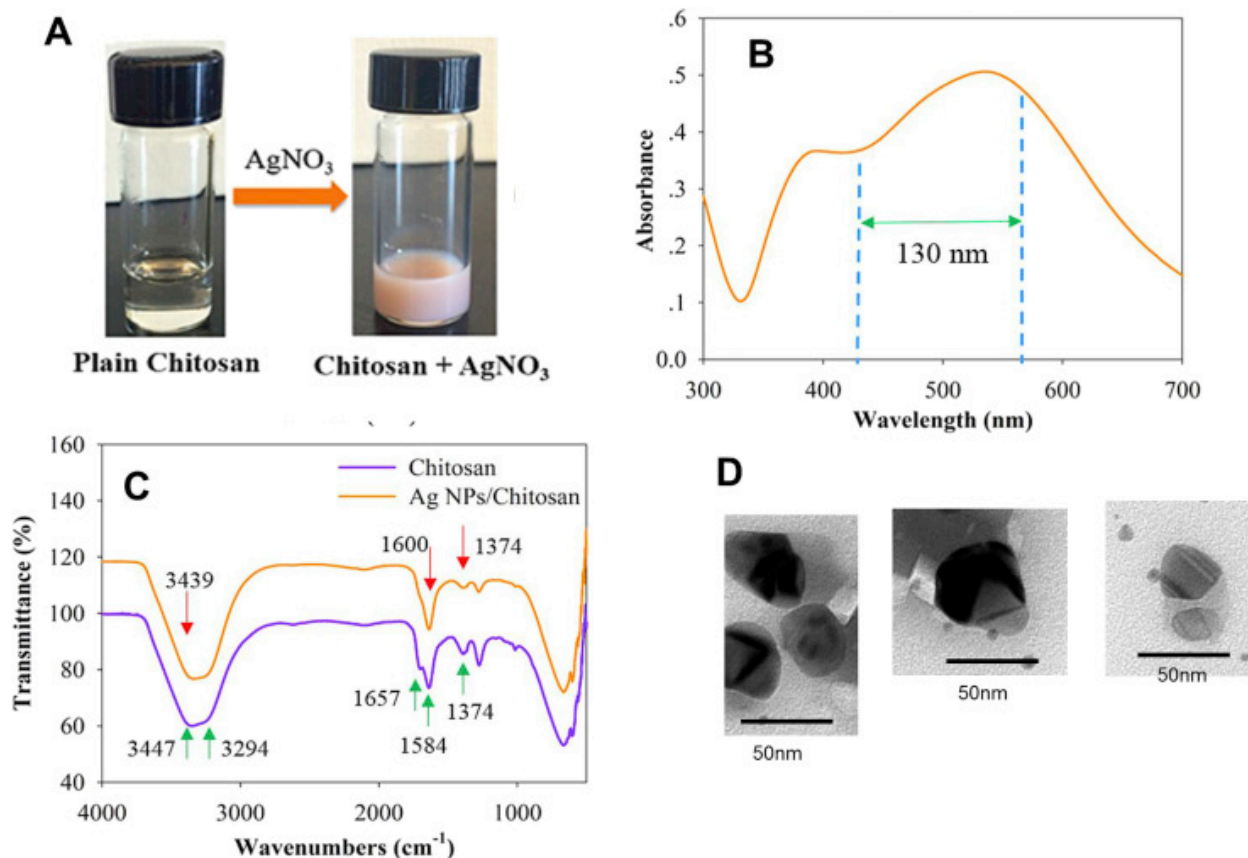


Fig. 1. (A) Vials containing chitin solution before (left) and after the addition of AgNO₃ (right), note the change in the color of the solution from clear to opaque with a purple hue. (B) UV–visible absorption spectra of AgNPs stabilized in chitosan. (C). FTIR spectra of AgNPs stabilized in chitosan (orange) and pure chitosan (blue). (D) TEM micrographs of cuboidal AgNPs produced by chitosan-based synthetic process.

By performing Fourier-transform infrared (FTIR) spectroscopy, we defined the specific functional groups within the chitosan polymer that are engaged in the AgNP synthetic reaction. Chitosan had FTIR absorption peaks at 3447 and 3294 cm⁻¹ due to the overlapping of hydroxyl (O–H) and amine (N–H) stretching bands, 1657 and 1584 cm⁻¹ due to amine (N–H) bending, and 1374 cm⁻¹ due to the C–H of the primary alcohol group in chitosan (Fig. 1C, blue line). In the FTIR spectrum of chitosan solution containing AgNO₃, the absorption bands at 1657 and 1584 cm⁻¹ that represent chitosan –NH₂ groups disappeared and were replaced by a single peak at 1600 cm⁻¹, which demonstrates the reaction of the Ag⁺ ion with the amine group (–NH) during and/or after the reduction to metallic silver (Fig. 1C, orange line); whether this represents a step in the nucleation process and/or a component of the stabilization of the nascent AgNPs remains unclear. However, we observed significant alteration in the shape and peak positions of –NH₂ and –OH groups at 3447 cm⁻¹, suggesting that there was an additional contribution of the amine group in this process, possibly in the stabilization of the nanoparticles [31]. TEM micrographs showed that the AgNPs produced by this method were cubical (Fig. 1D).

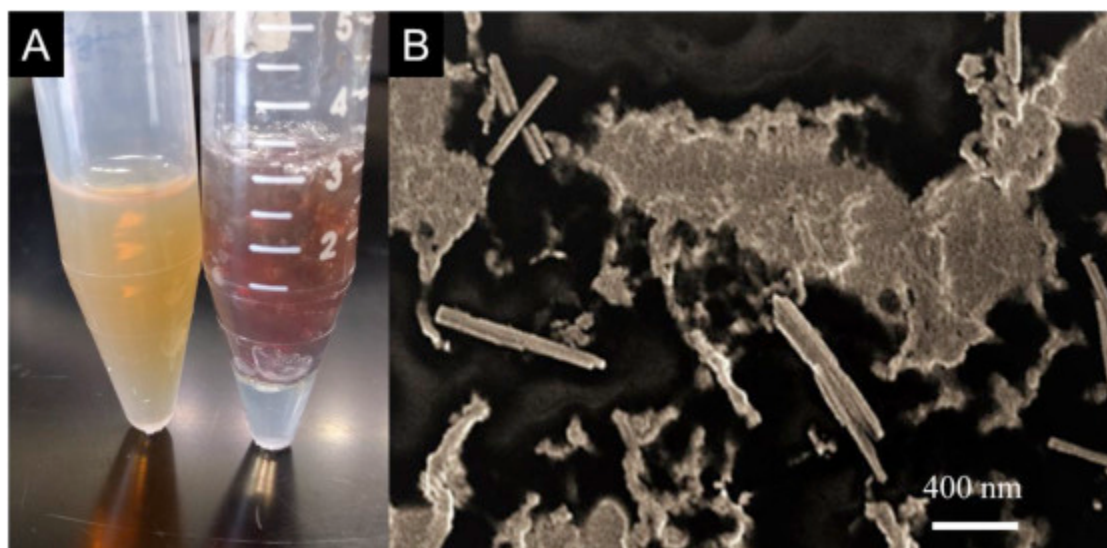


Fig. 2. pH dependence on chitosan-driven AgNP synthesis. (A) Left, an AgNO₃/chitosan solution of pH 3.0, color of the solution remains the same as that of an aqueous chitosan solution; right, an AgNO₃/chitosan solution of pH 9.0, color of the solution is purple, which is indicative of AgNP formation. Note the high viscosity of the solution as it remains clogged in the tube. (B) SEM micrograph of AgNPs formed in an AgNO₃/chitosan solution of pH 9.0, the AgNPs are rod shaped and not cuboidal as those prepared at pH 5.

2.2. Chitosan thin film-supported AgNW synthesis

The chitosan/AgNP solution was drop cast onto a clean glass substrate, which upon drying produced a 10- to 20- μm purplish thin film, which contained cuboidal AgNPs (Fig. 3B and D, Fig. S1). Chitosan thin films lacking AgNPs were clear and topologically smooth (Fig. 3A and C). After several days of incubation at room temperature, the SEM analysis of the AgNP-containing chitosan thin films demonstrated the presence of long, irregular AgNWs that erupted from the surface of the chitosan thin film (Fig. 3E). AgNWs were only observed on AgNP/chitosan thin films that had been starved of oxygen, either by smothering with a sputtered or plasma vapor-deposited layer of gold or by incubating an AgNP/chitosan thin film in a vacuum. Oxidation of the cuboidal AgNPs within the chitosan film by methanol washing [13], [32] resulted in a complete lack of AgNW formation further supporting this observation. Oxidative etching suppresses further the shape transformation of AgNPs in the polyol synthesis of AgNWs [33], and blocking oxidative etching is essential for the growth of AgNWs from AgNPs [34]. In this paper we report that, even in the solid state, when a Ag/chitosan thin film was subjected to oxygen starvation, the AgNPs on the film grew into AgNWs (Fig. 3). UV/vis spectroscopy of the Ag/chitosan thin film confirmed the presence of AgNWs (Figure S2). Analysis of SEM micrographs demonstrates that the AgNWs emerge from within the chitosan thin film (Fig. 3F, arrow). Unlike the AgNWs produced by previously described methods, such as PVP-mediated synthesis, that exhibit uniform 100-nm symmetric pentagonal rods [19], [20], chitosan-grown AgNWs displayed an irregular twisted/wandering morphology (Fig. 3E and F). This type of morphology is common for nanowires that form from self-growth and similar bottom up mechanisms commonly seen in semiconductor NW growth using ultrahigh vacuum and complex systems [35], [36]. The size of the chitosan nonlinear AgNWs had an average

length between 3 and 5 μm and diameter in the range of 100–150 nm (Fig. S3). Most processes that involve the formation of nanoparticle thin films or composite materials require two steps: the synthesis of the particles followed by a compositing step [20], [23], [37], [38]. The production of AgNW/chitosan nanocomposite material by this single pot, a self-seeding synthetic process, is simple and much more cost-effective than previously described nanocomposite synthetic methods.

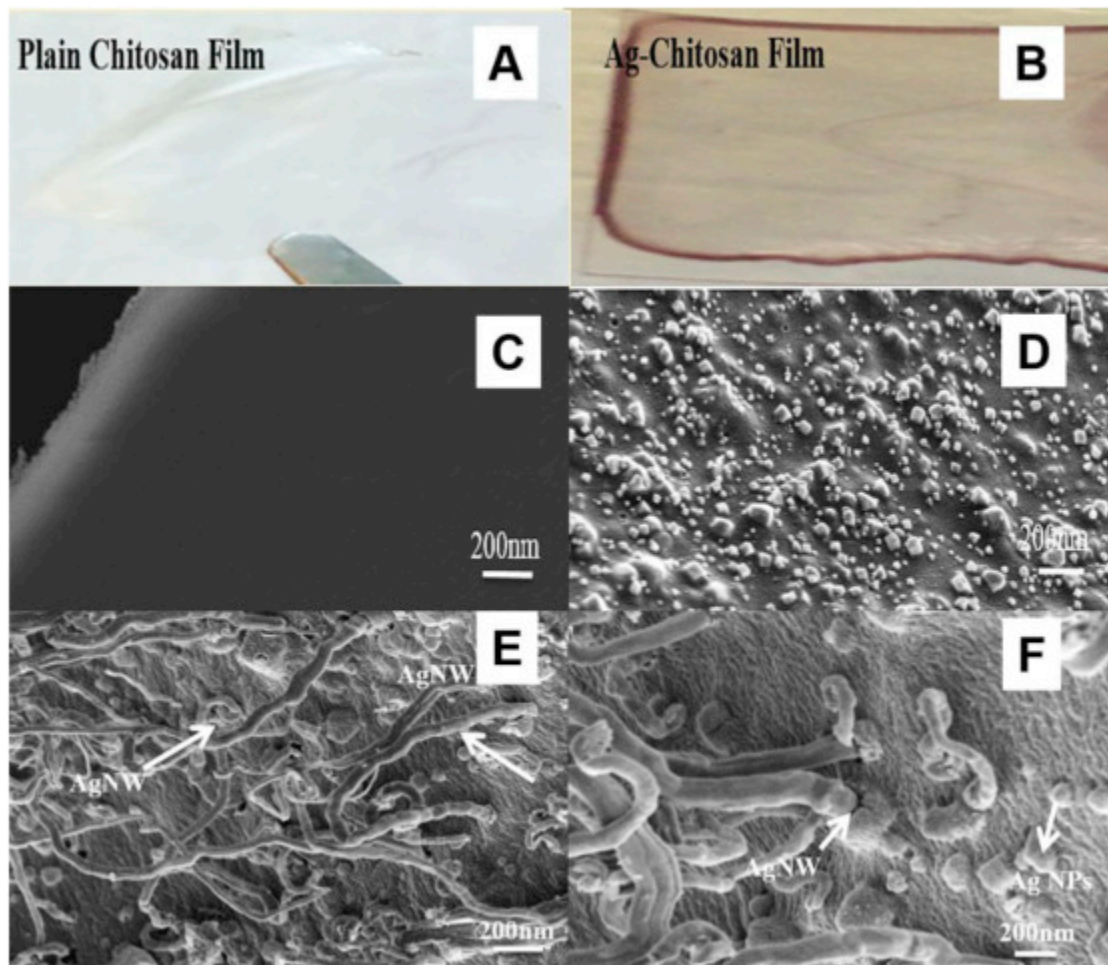


Fig. 3. Chitosan film with AgNPs and AgNWs. (A) 24-h Chitosan thin film without silver nanomaterials. (B) 24-h Chitosan thin film with AgNPs, note the purple color, which is indicative of silver nanomaterials. (C) A SEM micrograph of a 24-h chitosan thin film without any silver nanomaterials, note the smooth and unstructured surface. (D) A SEM micrograph of a 24-h chitosan thin film with AgNPs, note the presence of cuboidal nanomaterials emanating from the surface of the thin film matrix. (E) 96-h Chitosan thin film showing the presence of AgNWs and AgNPs (AgNW, arrow). (F) Higher magnification image of an AgNW that grows from the surface of the thin film (arrow), scale bar 200 nm.

Previous work has demonstrated that the polymer synthesis of crystalline AgNWs involves preferential growth from one crystal face, typically the $\langle 111 \rangle$, of a twinned faced crystalline seed particle [19], [20]. The XRD analysis of the AgNW/chitosan thin films showed that these nanowires display the crystal signatures of previous AgNWs (Fig. 4) [39]. To demonstrate that

chitosan-synthesized AgNWs also have a high crystallinity, we performed an XRD analysis on chitosan thin films that were produced with different concentrations of AgNO₃ (Fig. 4). It can be seen clearly from the XRD plot of the thin films formed from different concentrations of chitosan/AgNO₃ that with the increase in AgNO₃ concentration in the film, the growth orientation of AgNPs/NWs moved from $\langle 200 \rangle$ plane to $\langle 111 \rangle$ plane (Fig. 4A). Along these lines, the increase in concentration resulted in the generation of films that produced more AgNWs. This suggests that the AgNWs produced in this study are predominately $\langle 111 \rangle$ -oriented crystals similar to the AgNWs obtained by other synthetic processes [19], [20].

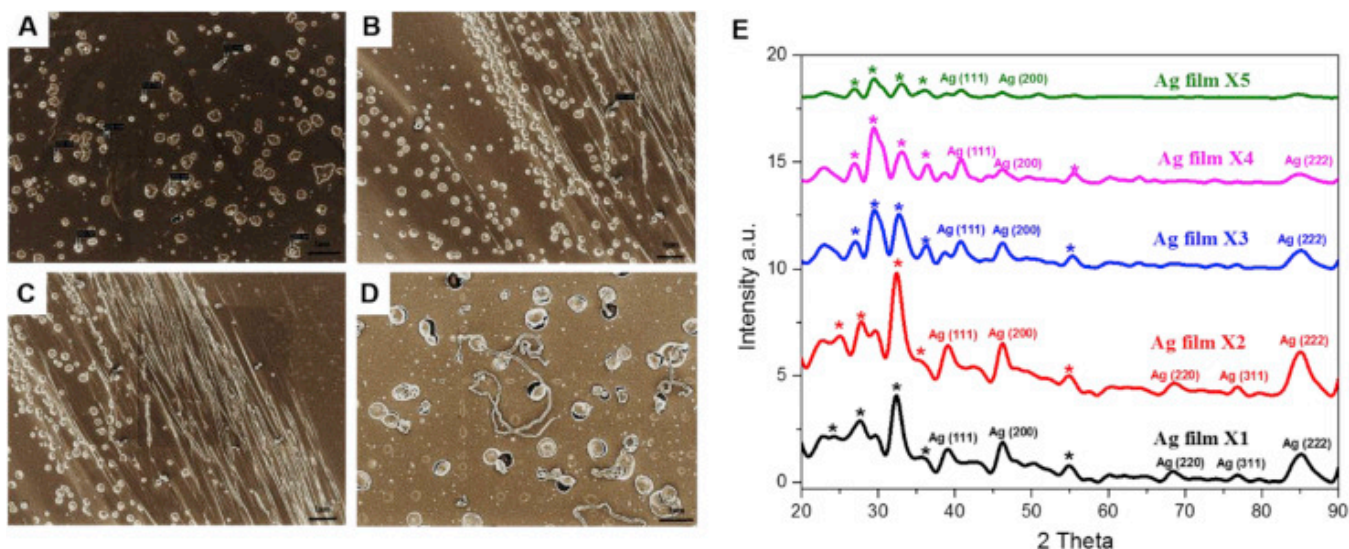


Fig. 4. SEM and XRD images of solid-state AgNW growth with different ratios of chitosan and AgNO₃. (A–D) SEM images of chitosan-based, solid-state AgNW growth after 48 h. (A) Chitosan/AgNO₃ ratio = 5:1, (B) chitosan/AgNO₃ ratio = 5:2, (C) chitosan/AgNO₃ ratio 5:3, (D) chitosan/AgNO₃ ratio 1:1; note that only this sample has significant generation of nanowires. (E) An overlay of five XRD spectra collected from a single AgNP-impregnated chitosan sample during AgNW growth: sample X1, ratio 5:1 chitosan/AgNO₃; sample X2, ratio 5:2 chitosan/AgNO₃; sample X3, ratio 5:3 chitosan/AgNO₃; sample X4, ratio 5:4 chitosan/AgNO₃; and sample X5, 1:1 chitosan/AgNO₃ ratio. Chitosan XRD 2 θ peaks are labeled with an *; the $\langle 222 \rangle$ predominates only in the highest ratios of chitosan and AgNO₃, which suggests that the crystallinity of the AgNWs is produced by this process.

Unlike the established methods of AgNW synthesis, which involve temperatures greater than 140 °C and organic solvents, chitosan thin film-mediated AgNW synthesis is performed at an ambient temperature (25 °C) and in an aqueous solution [19], [20]. As the film ages, smaller AgNPs within the film become less abundant because the AgNWs grow, which suggests that the AgNWs grow by Ostwald ripening process. Chitosan is produced by the deacetylation of the polysaccharide chitin, a major component of the cell wall of fungi and the cuticles of insects and other arthropods [40], [41], [42]. Chitin is the acetylated form of chitosan and the predominant structural component of the cuticles of arthropods and insects [41], [43]. Chitin is a stable polysaccharide that has been used extensively in food, pharmaceutical, and biomedical industries [44], and unlike chitosan, chitin is completely insoluble in aqueous solutions; chitin enabled us to test whether a similar AgNP/AgNW synthesis reaction was possible in the solid state. To determine whether chitin also facilitates the synthesis of AgNPs/AgNWs, we used

chitin scaffolds derived from the wings of the cicada *Magicicada septendecim* [41]. Purified wing chitin scaffolds retain the general morphology of the wings from which they were derived, although they lack all pigments (Fig. 5A).

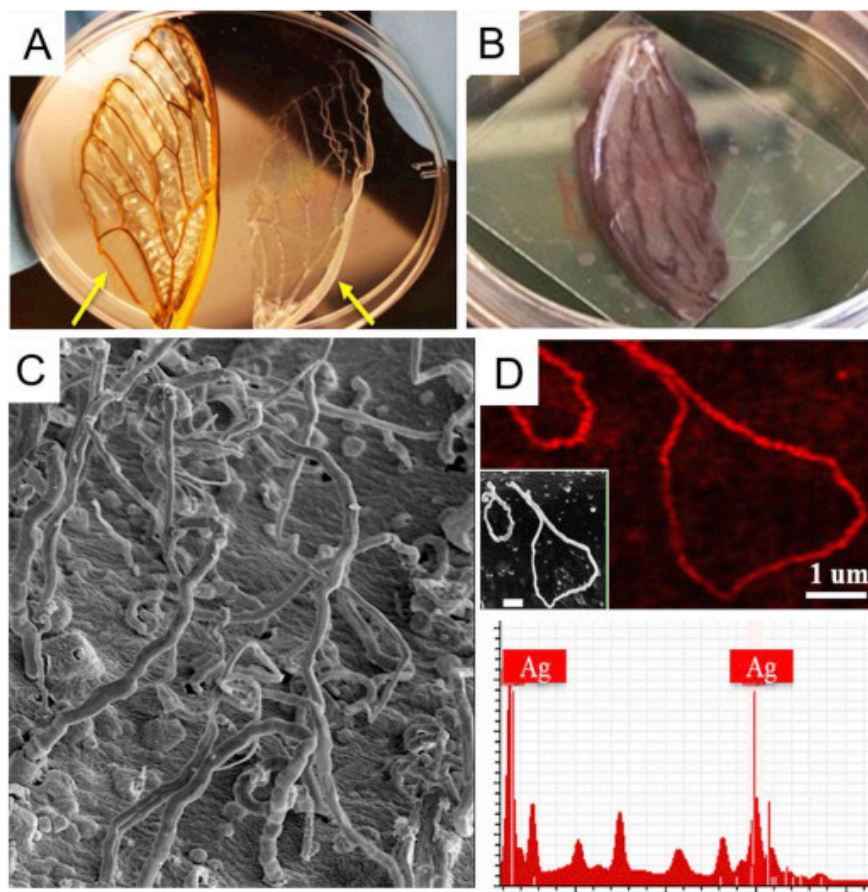


Fig. 5. AgNW growth on a purified insect chitin substrate. (A) Two forewings from the periodic cicada *M. septendecim*: the wing on the left is a wing before the removal of the protein/lipid cuticular matrix; the wing on the right is the chitin exoskeleton of a wing that has been processed, not the opaque, colorless appearance of the processed wing when compared to the native wing. (B) A purified chitin wing scaffold upon which AgNWs grow, note the purple color is indicative of silver nanomaterials. (C) A SEM image of AgNW growth from the chitin network of a purified cicada wing. (D) EDS/SEM analysis of AgNWs grown on a chitin network; inset, a SEM image of an AgNW; bottom, spectrograph of the emission peaks of AgNWs showing the emission of silver-specific X-rays.

Incubation of a purified wing chitin scaffold in a solution of [0.01 M] AgNO_3 resulted in the development of a purple hue to the clear/white scaffold, which is similar to the color changes that we observed in chitosan/ AgNO_3 thin films (Fig. 5B). Similar to the thin film formed from AgNPs/chitosan solution, AgNO_3 -treated wing surface possessed a large number of cuboidal AgNWs after oxygen starvation (achieved by sealing with a sputtered layer of Au) and exhibited AgNW formation (Fig. 5C). EDX/SEM analysis confirms that these wires, similar to those produced in a chitosan thin film, are also composed of silver (Fig. 5D). The FTIR analysis of chitin wing scaffold and a chitin wing scaffold with AgNPs/AgNWs demonstrated that the

interactions between silver and chitin are similar to the molecular-level interactions we observed between silver and chitosan and involved the nitro group (Supplemental Fig. S4). A one-pot synthesis of chitin/AgNW nanocomposites provides a new direction for the development of new chitin-based materials, especially for biomedical applications.

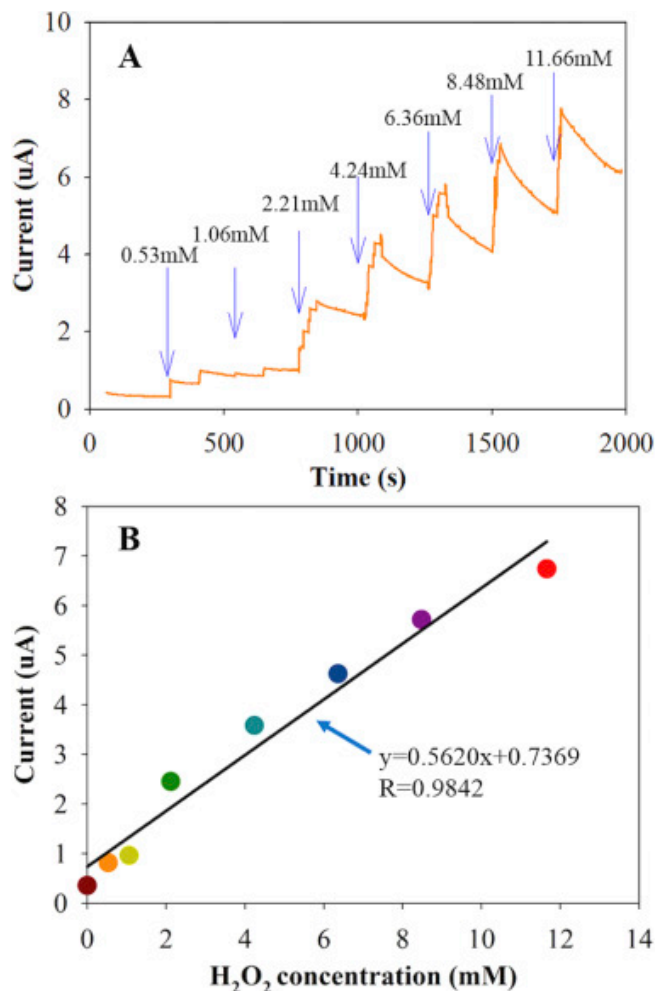


Fig. 6. Demonstration of the electrocatalysis and conductivity of chitosan/AgNW thin films by its application as a chemical sensor. (A) Chronoamperometry (CA) measurements at an applied voltage of 0.8 V with addition of different concentrations of H₂O₂. (B) Calibration curve for the CA measurements.

2.3. A chemical sensor application of AgNWs/chitosan thin films

Flexible thin films with a conductive nanomaterial, such as AgNWs, have applications in electronics [45], [46], [47], [48] and as sensors [49], [50]. To determine whether the chitosan/AgNW films are conductive, we used a hydrogen peroxide three-electrode testing system with a gold electrode connected to an AgNW-chitosan thin film (diameter of 2 mm) as the working electrode, a platinum wire as the counter electrode, Ag/AgCl as the reference electrode, and 5 mM PBS (pH 7.0) as the electrolyte solution (an applied voltage of 0.8 V). As a control, we used a thin-film working electrode made of chitosan only. In control experiments, we observed a steady state after 60 s with no increase in current in the presence of H₂O₂ (Fig. S5).

However, a device composed of a chitosan/AgNW working electrode was tested with an increase in H₂O₂ concentration from 0.53 to 11.66 mM, thus resulting in an increase in the current (Fig. 6A). This demonstrates that the enhanced current is due to the electrocatalysis of AgNWs to H₂O₂, resulting in the reduction of H₂O₂ into H₂O. After averaging the current over 240 s for individual concentrations of H₂O₂ (Fig. 5B), we observed a linear relationship between the current of the Ag-chitosan film electrode and H₂O₂ concentration from 0.53 to 11.66 mM ($R = 0.9842$) with a limit of detection of 94.3 μ M estimated by a signal-to-noise ratio of 3 ($3 \times$ standard error of 5 trials of blank sample/slope). This sensitive response is due to the high conductivity and good electrocatalytic activity of AgNW-chitosan films, indicating their potential application as H₂O₂ sensor and other sensors as well.

3. Conclusion

Chitosan and chitin are among the most common biopolymers on the planet and have many current applications in the food and biomedical industries. While most of these applications take advantage of the mechanical properties of chitosan and chitin, this work describes a new role of these polysaccharide materials in the synthesis of metallic nanoparticles that enable the one-pot synthesis of a flexible nanocomposite material. Chitosan and chitin facilitate a unique bottom-up growth of AgNPs and AgNWs on chitosan/chitin polymer thin films. This solid-state synthesis of silver nanomaterials is simple and environmentally friendly. The resulting AgNW chitin/chitosan nanocomposites are flexible and conductive and have potential in many applications including a broad variety of chemical detection systems.

4. Experimental

4.1. Chitosan and chitin sample preparation

Chitosan polymer (molecular weight: 150,000, 1.5% w/v), acetic acid, NaOH, and NaCl were purchased from Sigma-Aldrich (USA) and used as received without further purification. The Brood II Periodic cicada, *M. septendecim*, were collected locally in Greensboro, North Carolina; wings from these cicada were dissected carefully from the thorax and washed three times in DI water, and then, the protocol described in a previous work was followed [41]. After that, the dissected wing samples, after extracting chitin, were further dehydrated in an ethanol series 20%, 50% 70% 84%, 90%, and 95% for 10–15 min and in 100% ethanol overnight; then, the solvent was allowed to evaporate.

4.2. Synthesis of AgNPs/NWs in an aqueous chitosan solution

AgNO₃ (>99%) was purchased from Sigma Aldrich, and its solution of 10⁻² M was prepared. Chitosan (0.5 g, dissolved in 10 mL of 1% v/v acetic acid solution) and 0.2 M NaCl in 5 mL solution were added dropwise. Mixtures of chitosan and AgNO₃ solution were prepared with a ratio of 1:5 (by volume). The mixed sample solutions were ultrasonicated for 3–4 h to produce monodispersed nanoparticles. Further, the samples were drop casted and dried in an oven for about 10 min at 40 °C to form films and analyzed for various analytical characterizations.

4.3. Synthesis of AgNPs/NWs on chitin scaffold

The chitin scaffolds extracted from *M. septendecim* cicada wings were the source of chitin. A 10^{-2} -M AgNO_3 /0.2-M NaCl aqueous solution was added dropwise on to the chitin wing samples, and the samples were ultrasonicated for 3–4 h to disperse AgNPs.

4.4. Characterization techniques

The optical absorptions of chitosan and mixtures of colloidal solution of AgNO_3 (sample solutions) were evaluated in 10-mm optical path length quartz cuvettes of the ultraviolet–visible spectroscopy (UV–Vis spectroscopy, Varian Cary 6000i), followed by Fourier transform infrared spectroscopy (FTIR, Varian 670) measurements. To obtain the size of the synthesized AgNPs, a transmission electron microscope (TEM, Carl Zeiss Libra 120 Plus) was used. To obtain the results, a copper grid was plasma treated, and a drop of the sample solution was placed on the copper grid and dried using a vacuum drier before scanning the sample under TEM. Morphology including the shape and size of nanoparticles was viewed under a scanning electron microscope (SEM). Sample preparation and imaging for morphology study: The samples were placed on SEM sample pug. After drying, a 4-nm-thick gold layer was deposited on the samples using a Leica EM ACE200 with a real-time thickness monitoring quartz crystal microbalance. The SEM images were obtained using a Zeiss Auriga FIB/SEM. Scale bars were added using ImageJ software, followed by energy-dispersive X-ray spectroscopy analysis (Hitachi S-4800-I FESEM w/Backscattered Detector & EDX) to verify the presence of AgNPs/AgNWs.

Note. The authors declare no competing financial interest.

Funding sources. The North Carolina Biotechnology Center (NCBC) Biotechnology Research Grant (213-BRG-1209), an NIH grant to Dennis LaJeunesse (1R15EB024921-01), an NSF grant to Jianjun Wei (NSF-1511194), and the Southeastern Nanotechnology Infrastructure Corridor (SENIC) and the National Nanotechnology Coordinated Infrastructure (NNCI), which is supported by the National Science Foundation (ECCS-1542174).

Acknowledgment. This work was supported by the North Carolina Biotechnology Center (NCBC) Biotechnology Research Grant (213-BRG-1209 to Dr. Dennis LaJeunesse), an NIH grant to Dennis LaJeunesse (1R15EB024921-01), and by the generous support of Dr. James Ryan, the Joint School of Nanoscience and Nanoengineering, and the State of North Carolina. This work was performed at the JSNN, a member of the Southeastern Nanotechnology Infrastructure Corridor (SENIC) and the National Nanotechnology Coordinated Infrastructure (NNCI), which is supported by the National Science Foundation (ECCS-1542174).

Appendix A. Supplementary data

Supplementary data related to this article can be found at <https://doi.org/10.1016/j.mtnano.2018.04.002>.

References

- [1] M. Ahmadi, H. Mistry, B. Roldan Cuenya, Tailoring the catalytic properties of metal nanoparticles via support interactions, *J. Phys. Chem. Lett.* 7 (2016) 3519e3533.
- [2] B.R. Cuenya, Synthesis and catalytic properties of metal nanoparticles: size, shape, support, composition, and oxidation state effects, *Thin Solid Films* 518 (2010) 3127e3150.
- [3] J. Wang, H. Gu, Novel metal nanomaterials and their catalytic applications, *Molecules* 20 (2015) 17070.
- [4] G.V. Hartland, Measurements of the material properties of metal nanoparticles by time-resolved spectroscopy, *Phys. Chem. Chem. Phys.* 6 (2004) 5263e5274.
- [5] H.E. Saucedo, D. Mongin, P. Maioli, A. Crut, M. Pellarin, N.D. Fatti, F. Vallée, I.L. Garzón, Vibrational properties of metal nanoparticles: atomistic simulation and comparison with time-resolved investigation, *J. Phys. Chem. C* 116 (2012) 25147e25156.
- [6] G. Franci, A. Falanga, S. Galdiero, L. Palomba, M. Rai, G. Morelli, M. Galdiero, Silver nanoparticles as potential antibacterial agents, *Molecules* 20 (2015) 8856e8874.
- [7] B. Le Ouay, F. Stellacci, Antibacterial activity of silver nanoparticles: a surface science insight, *Nano Today* 10 (2015) 339e354.
- [8] J. Langer, S.M. Novikov, L.M. Liz-Marzán, Sensing using plasmonic nanostructures and nanoparticles, *Nanotechnology* 26 (2015).
- [9] R. Jin, Atomically precise metal nanoclusters: stable sizes and optical properties, *Nanoscale* 7 (2015) 1549e1565.
- [10] S. Marpu, S.S. Kolailat, D. Korir, B.L. Kamras, R. Chaturvedi, A. Joseph, C.M. Smith, M.C. Palma, J. Shah, M.A. Omary, Photochemical formation of chitosan-stabilized near-infrared-absorbing silver Nanoworms: a “Green” synthetic strategy and activity on Gram-negative pathogenic bacteria, *J. Colloid Interface Sci.* 507 (2017) 437e452.
- [11] T.K. Sau, A.L. Rogach, Nonspherical noble metal nanoparticles: colloid-chemical synthesis and morphology control, *Adv. Mater.* 22 (2010) 1781e1804.
- [12] X. Lu, M. Rycenga, S.E. Skrabalak, B. Wiley, Y. Xia, Chemical synthesis of novel plasmonic nanoparticles, *Annu. Rev. Phys. Chem.* 60 (2009) 167e192.
- [13] S. Irvani, H. Korbekandi, S.V. Mirmohammadi, B. Zolfaghari, Synthesis of silver nanoparticles: chemical, physical and biological methods, *Res. Pharmaceut. Sci.* 9 (2014) 385e406.
- [14] S. Guo, E. Wang, Noble metal nanomaterials: controllable synthesis and application in fuel cells and analytical sensors, *Nano Today* 6 (2011) 240e264.

- [15] A. Haider, I.K. Kang, Preparation of silver nanoparticles and their industrial and biomedical applications: a comprehensive review, *Adv. Mater. Sci. Eng.* 2015 (2015) 165257.
- [16] Q. Zhou, J. Lv, Y. Ren, J. Chen, D. Gao, Z. Lu, C. Wang, A green in situ synthesis of silver nanoparticles on cotton fabrics using Aloe vera leaf extraction for durable ultraviolet protection and antibacterial activity, *Textil. Res. J.* 87 (2017) 2407e2419.
- [17] N.I. Hulkoti, T.C. Taranath, Biosynthesis of nanoparticles using microbes-A review, *Colloids Surfaces B Biointerfaces* 121 (2014) 474e483.
- [18] V.K. Sharma, R.A. Yngard, Y. Lin, Silver nanoparticles: Green synthesis and their antimicrobial activities, *Adv. Colloid Interface Sci.* 145 (2009) 83e96.
- [19] Y. Sun, B. Mayers, T. Herricks, Y. Xia, Polyol synthesis of uniform silver nanowires: a plausible growth mechanism and the supporting evidence, *Nano Lett.* 3 (2003) 955e960.
- [20] T.N. Trung, V.K. Arepalli, R. Gudala, E.T. Kim, Polyol synthesis of ultrathin and high-aspect-ratio Ag nanowires for transparent conductive films, *Mater. Lett.* 194 (2017) 66e69.
- [21] H. Palza, Antimicrobial polymers with metal nanoparticles, *Int. J. Mol. Sci.* 16 (2015) 2099e2116.
- [22] N.M. Abbasi, H. Yu, L. Wang, A. Zain Ul, W.A. Amer, M. Akram, H. Khalid, Y. Chen, M. Saleem, R. Sun, J. Shan, Preparation of silver nanowires and their application in conducting polymer nanocomposites, *Mater. Chem. Phys.* 166 (2015) 1e15.
- [23] M. Anjidani, H. Milani Moghaddam, R. Ojani, Binder-free MWCNT/TiO₂ multilayer nanocomposite as an efficient thin interfacial layer for photoanode of dye sensitized solar cell, *Mater. Sci. Semicond. Process.* 71 (2017) 20e28.
- [24] A.M. Stephan, T.P. Kumar, M.A. Kulandainathan, N.A. Lakshmi, Chitin-incorporated poly(ethylene oxide)-based nanocomposite electrolytes for lithium batteries, *J. Phys. Chem. B* 113 (2009) 1963e1971.
- [25] J. Wen, X. Tan, Y. Hu, Q. Guo, X. Hong, Filtration and electrochemical disinfection performance of PAN/PANI/AgNWs-CC composite nanofiber membrane, *Environ. Sci. Technol.* 51 (2017) 6395e6403.
- [26] T. Quang Trung, H. Tran My Hoa, T. Duc Tai, T. Van Tam, N. Nang Dinh, Synthesis and application of graphene-silver nanowires composite for ammonia gas sensing, *Adv. Nat. Sci. Nanosci. Nanotechnol.* 4 (2013) 045012.
- [27] L. Da Sacco, A. Masotti, Chitin and chitosan as multipurpose natural polymers for groundwater arsenic removal and AS₂O₃ delivery in tumor therapy, *Mar. Drugs* 8 (2010) 1518e1525.

- [28] C.K.S. Pillai, W. Paul, C.P. Sharma, Chitin and chitosan polymers: chemistry, solubility and fiber formation, *Prog. Polym. Sci.* 34 (2009) 641e678.
- [29] S. Hajji, I. Younes, O. Ghorbel-Bellaaj, R. Hajji, M. Rinaudo, M. Nasri, K. Jellouli, Structural differences between chitin and chitosan extracted from three different marine sources, *Int. J. Biol. Macromol.* 65 (2014) 298e306.
- [30] D. Wei, W. Sun, W. Qian, Y. Ye, X. Ma, The synthesis of chitosan-based silver nanoparticles and their antibacterial activity, *Carbohydr. Res.* 344 (2009) 2375e2382.
- [31] S. Govindan, E.A.K. Nivethaa, R. Saravanan, V. Narayanan, A. Stephen, Synthesis and characterization of chitosan/silver nanocomposite, *Appl. Nanosci.* 2 (2012) 299e303.
- [32] Y. Zheng, J. Zeng, A. Ruditskiy, M. Liu, Y. Xia, Oxidative etching and its role in manipulating the nucleation and growth of noble-metal nanocrystals, *Chem. Mater.* 26 (2014) 22e33.
- [33] A. Amirjani, D.H. Fatmehsari, P. Marashi, Interactive effect of agitation rate and oxidative etching on growth mechanisms of silver nanowires during polyol process, *J. Exp. Nanosci.* 10 (2015) 1387e1400.
- [34] Y. Xia, Y. Xiong, B. Lim, S.E. Skrabalak, Shape-controlled synthesis of metal nanocrystals: simple chemistry meets complex physics? *Angew. Chem. Int. Ed.* 48 (2009) 60e103.
- [35] C.-Y. Wang, Y.-C. Hong, Z.-J. Ko, Y.-W. Su, J.-H. Huang, Electrical and optical properties of Au-Catalyzed GaAs nanowires grown on Si (111) substrate by molecular beam epitaxy, *Nanoscale Res. Lett.* 12 (2017) 290.
- [36] T. Rieger, M. Luysberg, T. Schäpers, D. Grützmacher, M.I. Lepsa, Molecular beam epitaxy growth of GaAs/InAs core-shell nanowires and fabrication of InAs nanotubes, *Nano Lett.* 12 (2012) 5559e5564.
- [37] A.P. Mathew, M.P.G. Laborie, K. Oksman, Cross-linked chitosan/chitin crystal nanocomposites with improved permeation selectivity and pH stability, *Biomacromolecules* 10 (2009) 1627e1632.
- [38] H.F. Giraldo Mejía, L. Yohai, A. Pedetta, K. Herrera Seitz, R.A. Procaccini, S.A. Pellice, Epoxy-silica/clay nanocomposite for silver-based antibacterial thin coatings: synthesis and structural characterization, *J. Colloid Interface Sci.* 508 (2017) 332e341.
- [39] Y. Zhang, G. Gao, Q. Qian, D. Cui, Chloroplasts-mediated biosynthesis of nanoscale Au-Ag alloy for 2-butanone assay based on electrochemical sensor, *Nanoscale Res. Lett.* 7 (2012).
- [40] M. Bajaj, A. Freiberg, J. Winter, Y. Xu, C. Gallert, Pilot-scale chitin extraction from shrimp shell waste by deproteination and decalcification with bacterial enrichment cultures, *Appl. Microbiol. Biotechnol.* (2015).

- [41] R. Chandran, L. Williams, A. Hung, K. Nowlin, D. LaJeunesse, SEM characterization of anatomical variation in chitin organization in insect and arthropod cuticles, *Micron* 82 (2016) 74e85.
- [42] L. Zhao, Y. Wu, S. Chen, T. Xing, Preparation and characterization of crosslinked carboxymethyl chitin porous membrane scaffold for biomedical applications, *Carbohydr. Polym.* 126 (2015) 150e155.
- [43] I. Younes, M. Rinaudo, Chitin and chitosan preparation from marine sources. Structure, properties and applications, *Mar. Drugs* 13 (2015) 1133e1174.
- [44] I. Hamed, F. Özogul, J.M. Regenstein, Industrial applications of crustacean byproducts (chitin, chitosan, and chitooligosaccharides): a review, *Trends Food Sci. Technol.* 48 (2016) 40e50.
- [45] M. Amjadi, A. Pichitpajongkit, S. Ryu, I. Park, 2014 IEEE 27th International Conference on Micro Electro Mechanical Systems (MEMS), 2014, pp. 785e788.
- [46] Y. Zhou, F. Liu, High-performance polyimide nanocomposites with core-shell AgNWs@BN for electronic packagings, *Appl. Phys. Lett.* 109 (2016) 082901.
- [47] S. Lee, S. Shin, S. Lee, J. Seo, J. Lee, S. Son, H.J. Cho, H. Algadi, S. Al-Sayari, D.E. Kim, T. Lee, Ag nanowire reinforced highly stretchable conductive fibers for wearable electronics, *Adv. Funct. Mater.* 25 (2015) 3114e3121.
- [48] G.-W. Huang, H.-M. Xiao, S.-Y. Fu, Wearable electronics of silver-nanowire/poly(dimethylsiloxane) nanocomposite for smart clothing, *Sci. Rep.* 5 (2015) 13971.
- [49] C.-J. Lee, K.H. Park, C.J. Han, M.S. Oh, B. You, Y.-S. Kim, J.-W. Kim, Crack-induced Ag nanowire networks for transparent, stretchable, and highly sensitive strain sensors, *Sci. Rep.* 7 (2017) 7959.
- [50] X. Shuai, P. Zhu, W. Zeng, Y. Hu, X. Liang, Y. Zhang, R. Sun, C.-p. Wong, Highly sensitive flexible pressure sensor based on silver nanowires-embedded polydimethylsiloxane electrode with microarray structure, *ACS Appl. Mater. Interfaces* 9 (2017) 26314e26324.